Journal of Polymers and the Environment (2022) 30:3203–3208
https://doi.org/10.1007/s10924-022-02401-9

ORIGINAL PAPER

The Bovine Serum Albumin Coated Copper Oxide Nanoparticle for Curcumin Delivery in Biological Environment: *In-vitro* Drug Release

Tahmineh Atloo[1] · Ramin Mohammadkhani[1] · Ali Mohammadi[2] · Kasra Arbabi Zaboli[4] · Saeed Kaboli[4] · Hossein Rahimi[4] · Hamed Nosrati[2,3] · Hosein Danafar[2,3]

Accepted: 9 February 2022 / Published online: 22 March 2022

Abstract
The copper oxide nanoparticles (CuO NPs) were synthesized by a simple method and then coated with the bovine serum albumin (BSA) to form CuO@BSA NPs. Finally, curcumin (CUR) as an anticancer drug was loaded to the CuO@BSA NPs. The characterization of nanoparticles was carried out by Fourier-transport infrared (FT-IR), ultraviolet-visible (UV-vis), transmission electron microscopy (TEM), and atomic force microscopy (AFM) analysis. It was found that the synthesized CuO@BSA-CUR nanoparticles were spherical with a particle size of 20–30 nm. Also, the result of drug release in the biological environment showed that maximum drug release for this nanocarrier in pH of 7.4 was measured 72% after 48 h. The cytotoxicity of CuO@BSA-CUR against the MDA-MB-231 breast cancer cell line was studied by MTT assay test. The results indicated that CuO@BSA-CUR nanoparticles have a remarkable anticancer effect on breast cancer cell line.

Keywords Copper oxide · Bovine serum albumin · Curcumin · MTT assay

Introduction

Cancer is defined as an unregulated cell growth and the invasion and spread of cells from the original site to other parts of the body [1]. One of the most common deaths in recent decades is related to cancer, which according to the Health Organization, about 13% of deaths are due to cancer [2]. To treat cancer, the common treatments such as surgery, chemotherapy, radiation therapy are applied. One of the main difficulties in chemotherapy is the biodistribution of the chemotherapeutic compound, which can damage to normal cells [3]. To overcome this drawback limit, a carrier system in the form of nanoparticles must be designed that can selectively deliver cytotoxic doses of therapeutic agents inside cancer cells [4].

A nanoparticle is usually defined as a particle of matter with a structure of small size between 1 and 100 nm in diameter, which due to the size effect shows specific properties and functions [5]. Interest in the design and development of nanoparticles for applications in a wide range of various fields has continued to grow in the past decade due to their unique properties of the physical and chemical [6–9]. In particular, they have achieved significant attention mainly in biomedical fields, especially applications in biomedical fields, especially as a new method in the development of drug delivery systems [10, 11].

Among nanocarriers that are used in various fields of medicine and treatment, nanocrystalline semiconductors particles have been considered in drug delivery due to their unique properties such as non-toxicity, increased activity, large high surface-to-volume ratio, high magnetic conductivity, and solubility [12]. Copper oxide as a suitable option among transition metal oxides in common form cupric

✉ Ramin Mohammadkhani
ramin6072@gmail.com

✉ Hosein Danafar
danafar@zums.ac.ir

1 Department of Physics, Faculty of Science, University of Zanjan, 45371-38791 Zanjan, Iran

2 Zanjan Pharmaceutical Biotechnology Research Center, Zanjan University of Medical Sciences, Zanjan, Iran

3 Department of Pharmaceutical Biomaterials, School of Pharmacy, Zanjan University of Medical Sciences, Zanjan, Iran

4 Department of Medical Biotechnology, School of Medicine, Zanjan University of Medical Sciences, Zanjan, Iran

oxide (CuO) possesses an attractive advantage. CuO NPs are relatively cheap which easily mixed with polymers and relatively stable because of both chemical and physical properties. They are used as antiinfective agents against drug-resistant bacteria while keeping acceptable biocompatibility and small dimensions. Also, CuO has applications in magnetic storage media, electronics, sensors, batteries [13–15].

Coating and modification of the surface of copper oxide nanoparticles with various biocompatible and biodegradable are important in order to obtain nanoparticles with suitable stability [16]. Bovine serum albumin (BSA) has received much attention in drug delivery for coating nanoparticles surfaces due to its properties like biodegradability, nontoxicity, high chemical stability, easy availability, and long half-life [17–20]. BSA is a common protein and the main protein in the plasma of blood. It is a globular heart-shaped protein that possesses 585 amino acids and a molecular mass of 66 kDa. Due to the nontoxic, biocompatible, and biodegradable properties of albumin, it is used as a proper drug carrier. Hence, BSA has attracted significant interest in the field of nano-biotechnology and protein-based nanoparticles which are applied as a matrix for the physical loading of different drugs [21].

Curcumin (CUR) is a natural remedy and the main components of turmeric spice include properties such as antioxidant, anti-inflammatory. It is also a liposoluble compound that can be easily dissolved into an organic solvent such as methanol, ethanol, and acetone [22]. Also, according to the preclinical data of the anticancer property of curcumin, it has concerned significant attention in drug delivery systems for cancer research [23–25]. In 2017, Xie and their colleagues developed nanoparticles that contain the anticancer drug curcumin for chemotherapy and photothermal treatment of cancer cells. The results showed that the synthesized nanoparticles containing curcumin can accumulate in the tumor and also protect normal cells from the effects of radiation therapy [25].

In this study, first copper oxide nanoparticles were produced by and next their surface was coated with BSA. Afterward, the CuO@BSA was utilized for loading the natural anticancer drug of curcumin which is called CuO@BSA-CUR. The morphology and characterization of the samples were investigated by FT-IR, UV-vis, TEM, AFM techniques. Finally, the maximum release of the drug was evaluated by dialysis bag. The cytotoxicity of CuO@BSA-CUR NPs on the MDA-MB-231 cell line was evaluated, which is an epithelial and human breast cancer cell line in medical research laboratories.

Materials and Methods

Materials

Copper sulfate, sodium hydroxide, bovine serum albumin, Dimethyl sulfoxide (DMSO), 3-(4,5-dimethylthiazol-2-yl)-2,5-diphenyltetrazolium bromide (MTT), and curcumin were obtained from Sigma-Aldrich (St. Louis, USA). Other chemicals and solvents were gifted from Emerat Chimi Company (Tehran, Iran).

Synthesis of Copper Oxide (CuO)

First, 40 mg of copper sulfate ($CuSO_4$) was added to 6 mL of water (H2O) and placed on a magnetic stirrer at room temperature. Afterward, 1 mL of acetic acid ($C_2H_4O_2$) was added to the above solution. In the next step, 120 mg of NaOH (sodium hydroxide) was added to the solution and placed on the magnetic stirrer for 24 h at room temperature to yield a brown color product. Then, after 24 h, the product was purified by centrifugation.

Synthesis of Final Nanoparticles (CuO@BSA-CUR)

In order to obtain an aqueous solution of a mixture of 8 mg CuO and 32 mg BSA was added to 10 mL deionized water and stirred for 15 min at room temperature. Then CUR solution (10 mg of CUR in 1.5 mL of ethanol) was added dropwise to the above solution. The obtained solution was stirred by a magnetic stirrer for 24 h, and to purify was centrifuged for 15 min at 21,000 rpm for four cycles. In order to dry the resulting solution, it was placed in an oven at 40 ° C for 48 h.

Characterization

Determine the Particle Size

The size and morphology of the sample of CuO@BSA-CUR NPs were characterized by transmission electron microscopy. (TEM, Cambridge 360–1990 Stereo Scan Instrument-EDS, CA).

FT-IR Analysis

The chemical structure of the samples was determined by FT-IR (Bruker, Tensor 2, Biotage, Germany). Transparent pills were prepared by mixing and grinding 2 mg of selected samples with 200 mg of powder KBr and then compressing the resulting powder under a pressure of 12 Ton. The FT-IR spectra of all samples can record from the wavenumber 400-4,000 cm^{-1}.

UV-vis Analysis

Optical analysis of CUR, CuO@BSA, and CuO@BSA-CUR aqueous was performed using the UV-vis spectrum (analytikjena model SPECORD 210 PLUS, Germany) in the wavelength range of 200–800 nm. Every sample was diluted with 1.5 mL deionized water and kept in a quarts cell.

AFM Analysis

The surface topography of the aqueous solution of the samples was determined by an atomic force microscope (AFM, Ara Research Company, Nano Expert, Model No. 0101/A, Iran). One droplet of the sample was placed on a freshly cleaved mica substrate (1 cm^2) and dried in the air, AFM analysis was carried out in contact AFM mode.

Determine of Loading Efficiency

For the curcumin-loading experiment, 400 µL of the final sample (CuO@BSA-CUR) was dispersed in 1 mL of ethanol and then shaken in a shaker incubator (100 rpm) at 37 °C for 24 h. The suspension was centrifuged for 15 min at 13,000 rpm. Drug loading was calculated was measured using UV-vis spectroscopy at the wavelength of 420 nm.

The amount of loaded CUR was determined as follows:

$$Drug\ Loading\ (\%) = \frac{weight\ of\ drug\ in\ nanoprticles}{weight\ of\ drug\ loaded\ nanoprticles} \times 100$$

Drug Release Study

After loading of the drug on nanoparticles, the release of curcumin from CuO@BSA-CUR was evaluated at pH = 7.4 using a dialysis process. Briefly, 200 µL of the CuO@BSA-CUR was dispersed with 1 mL of phosphate buffer solution (PBS) then was transported to a dialysis tube with 12 kDa molecular weight cut off. The dialysis bag was immersed in 35 mL of 65% PBS solution (PBS: ethanol (65:35)). The sample was then stirred in an incubator at 37 °C and 100 rpm. At predetermined time intervals, 1 mL of the dialysate was taken out and replaced by 1 mL new PBS. The amount of released CUR was measured using UV-vis spectroscopy at the wavelength of 420 nm. This study three times was repeated.

Cell Viability Test

In vitro cell viability was assigned via MTT assay. The cells were cultured in 96-well plates and after 24 h time periods, the cells were treated with different concentrations of the materials and culture medium as control. The cytotoxicity effect of synthesized nanoparticles was performed at various concentrations of 8, 16, 32, and 64 µg/mL of free CUR and CuO@BSA-CUR NPs and incubated for 48 h. Then, after 48 h the culture medium was removed and then 20 µL of MTT with a concentration of 5 mg/mL was added to each well and incubated for 4 h. Next, after 4 h incubation, 150 µL of DMSO was added to each well, and absorbance reading of each well was performed at 570 nm. Finally, the absorbance ratio of the number of surviving cells in treated samples was compared with the control group cells. After mild shaking for 15 s, the absorbance of treated wells was compared to the control group.

Results and Discussion

Characterization of CuO@BSA-CUR

FT-IR Analysis

To confirm the loading of CUR on CuO@BSA NPs, Infrared absorption spectra of compositions of pure CUR, CuO@BSA NPs, and CUR loaded CuO@BSA NPs were performed. The results were shown in Fig. 1. Characteristic peaks for pure CUR were identified in the regions of 3437 cm^{-1} and 1628 cm^{-1} (C = O). The absorption peak at 3437 cm^{-1} can be attributed to the stretching vibrations of hydroxyl functional groups (O-H) while the peak at 1628.40 cm^{-1} is due to the molecular stretching of the carbonyl group (C = O). In addition, the absorption peak 1282 cm^{-1} is related to C-O for the enol structure of curcumin. FT-IR spectra of CuO@BSA showed characteristic peaks at 1653 cm^{-1}, 3423 cm^{-1}, 2926 cm^{-1} which are assigned to the C = O carbonyl groups vibrations, the stretching vibrations of O-H and C-H, respectively. The absorption spectrum of CuO@BSA-CUR nanoparticles depicts the peaks in the region of 1654 cm^{-1} and 3431 cm^{-1} correspond to the flexural vibrations of the C = O carbonyl groups and the N-H amine groups, respectively. It can be noticed from Fig. 1 that the wavenumber in the bond of the carbonyl group (C = O) for CuO@BSA-CUR structure shifts towards higher wavenumber compared with free CUR. This shifting and increase in the wavenumber of this band are attributed to the surface bond between CUR and CuO@BSA.

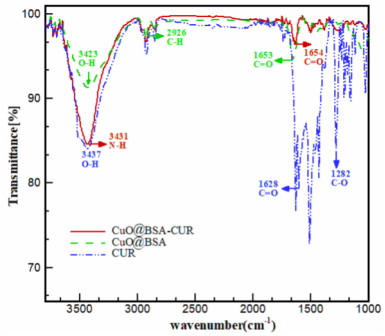

Fig. 1 FT-IR spectra of CUR, CuO@BSA and CuO@BSA-CUR

UV-vis Spectrophotometry Analysis

UV-vis spectroscopy was used to determine the amount of CUR loaded on the surface of CuO@BSA NPs. Therefore, as shown in Fig. 2 the UV-vis absorption spectrum of CUR, CuO@BSA and CuO@BSA-CUR were performed. There are three peaks around 235 nm, 275 nm, and 420 nm in the spectrum of CUR. In the UV-vis spectrum of CuO@BSA, a characteristic peak is observed around 260 nm. The appearance of two absorption peaks at wavelengths around 265 nm, 400 nm in the UV-Vis spectrum of CuO@BSA-CUR indicates the characteristic peaks of CUR possess a noticeably blue shift after loading CUR to CuO@BSA and compared to the characteristic of CUR spectrum, the maximum wavelengths of CUR were shifted toward smaller wavelengths. These results confirm the loading CUR on CuO@BSA NPs, resulting in the formation of CuO@BSA-CUR nanocomposite.

TEM of CuO@BSA-CUR NPs

TEM analysis was used to determine the size and morphology of the produced nanoparticles. As shown in Fig. 3, the TEM image of CuO@BSA-CUR NPs indicates that the nanoparticles are almost spherical in shape and have uniform morphology. The average diameter of the as-obtained NPs was around 25 nm. Particle size has a key role in the biological performance of sub-micron size delivery systems. According to previous reports, the optimal size of NPs for treating tumors is around 100 nm. Hence, the NPs with micron-sized aggregates will affect nanoparticles properties, which, in turn, will affect their performance to kill cancer cells. Also, micron-size aggregates can be caused rapid membrane damage, resulting in acute cell kill [26]. According to the size of the synthesized NPs here, they can therefore be used in biopharmaceutical applications.

AFM Analysis

One of the methods used to determine the surface topography is AFM analysis. As shown in Fig. 4, in order to evaluate the coating of BSA and CUR on the rough surface CuO NPS, the morphology of CuO@BSA and CuO@BSA-CUR NPs was performed with the use of AFM. According to our previous work, the thickness of CuO NPs has 12 nm. Figure 4a representing the AFM height profile characterized with the Z sign expresses that the thickness of BSA-coated CuO is around 20 nm. A noticeable geometry deformation in Fig. 4b emerges, which clearly declares the CUR can affect the topography of CuO@BSA surface and the thickness of the final sample reaches 42 nm. Hence after mixing BSA and CUR, the particle size distribution and morphology of CuO NPs remarkably changes. Therefore, a comparison of Fig. 4 (a-b) exhibits that the radius of CuO NPs increases at all structures. This finding confirms that BSA and CUR interact with CuO NPs and adsorb on their surfaces for the formation of a CuO@BSA-CUR nanocarrier.

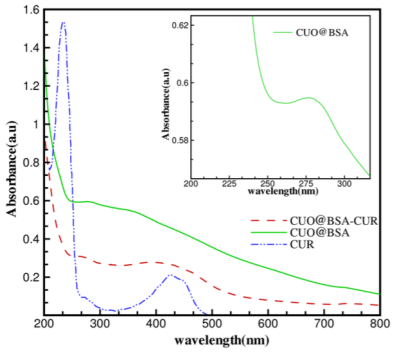

Fig. 2 UV-vis absorption spectrum of CUR, CuO@BSA and CuO@BSA-CUR. Inset shows UV-vis spectrum of CuO@BSA around the absorption peak

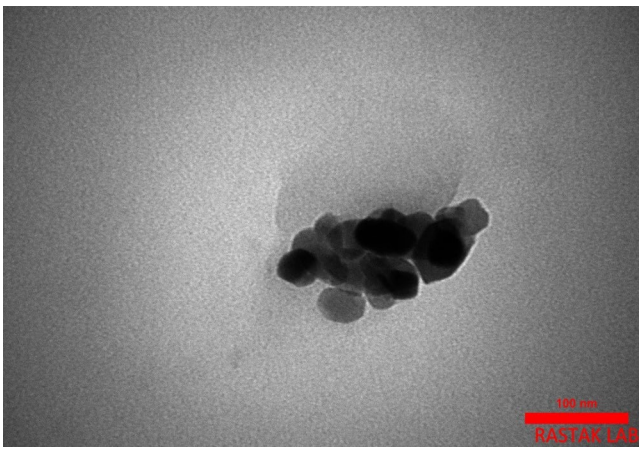

Fig. 3 TEM images of CUR loaded on CuO@BSA

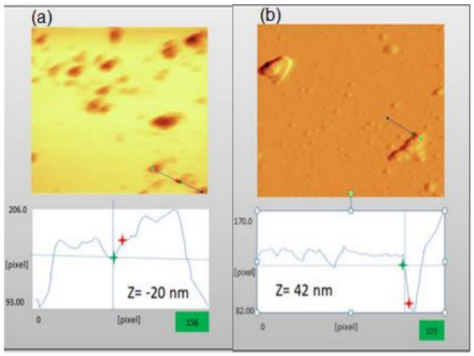

Fig. 4 AFM of (a) CuO@BSA (b) CuO@BSA-CUR

Investigation of Drug Release in Neutral Medium

In the design of the modern delivery systems, loading and controlled drug release is a very important issue, which can be dependent on parameters such as pH, temperature and etc. In the present study, CUR was utilized as an anticancer drug for loading and controlled release behavior of CuO@BSA as a nanocarrier. UV-vis spectrophotometry was utilized to investigate the loading amount of the CUR on the surface of NPs. The CUR standard curve with different concentrations was recorded at 420 nm. The method produced linear responses throughout the CUR concentration range of 0. 007–0.05 µg mL-1. A typical linear regression equation of the method was: $y = 0.1119\ x - 0.0031$, with x and y representing CUR concentrations in µg mL-1 and the corresponding peak absorbance, respectively, and the coefficient of determination of the linear regression (R^2) of 0.986. The loading efficiency of CUR was $14.3 \pm 1.27\%$. The amount of curcumin released from the surface of NPs was measured by UV-vis spectroscopy at the wavelength of 420 nm. As shown in Fig. 5, the cumulative release drug of CUR from the nanocarrier in physiological conditions (pH = 7.4) was about 70% after 40 h. The released drug from CuO@BSA-CUR NPs was slower and reaches its maximum value (72%) after 48 h and can be sustained over 50 h.

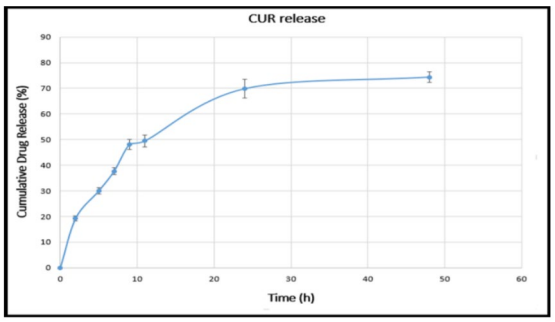

Fig. 5 The release profiles of the CUR from NPs at pH of 7.4

Anti-Cancer Activity Assay

The *in vitro* anticancer effects of free CUR, CuO@BSA, and CuO@BSA-CUR NPs against human breast cancer cells (MDA-MB-231) were estimated were using MTT assay (Fig. 6). As shown in Fig. 6, the cell viability has been plotted as a function of CUR, CuO@BSA NPs, and CuO@BSA-CUR NPs at various concentrations. The data exhibit that cell toxicity is directly commensurate to CUR concentration. The results of MTT cytotoxicity test on MDA-MB-231 cells showed that by enhancing concentration, the toxicity of the free CUR and CuO@BSA-CUR NPs increases in compared control, whereas CuO@BSA NPs with similar concentrations do not exhibit any toxic effect on treated cells in various concentrations after 48 h incubation time. These studies specify that CuO@BSA-CUR NPs have a very remarkable anticancer effect, for breast cancer cell lines.

Conclusions

In summary, CuO NPs were designed and successfully prepared by a facile method. Afterward, for preparing CuO@BSA-CUR NPs, the surfaces of CuO NPs were functionalized with BSA via simple mixing. Then these NPs loaded with curcumin. Afterward the synthesis, the NPs were characterized with UV-vis, FT-IR, AFM, and TEM techniques.

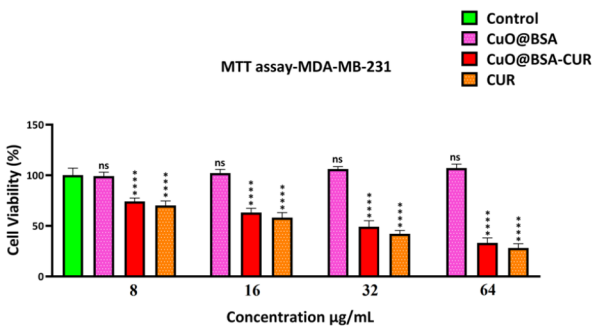

Fig. 6 Cytotoxicity analysis of free CUR, CuO@BSA, and CuO@BSA-CUR after incubation 48 h on cancer cells at pH = 7.4

The results demonstrated the successful synthesis of CuO@BSA-CUR NPs. The results of curcumin release in the biological environment at pH = 7.4 showed that after 40 h about 70% of curcumin was released and after 48 reaches 72% which is the maximum value of the release. The results related to the cellular cytotoxicity study exhibited no inhibitive effects of CuO@BSA NPs on cancer cells of MD-MB-231, while CuO@BSA-CUR composite pronounced high cytotoxicity effect. As a result, although CuO NPs in drug delivery systems are limited due to their toxicity effect, after mixing with BSA and having acceptable biocompatibility this drawback limit can be removed. Hence, the use of CuO NPs loaded with anti-cancer drugs becomes more apparent in *in-vitro* drug delivery studies.

Acknowledgements The work presented here is the result of the Master's thesis of Tahmineh Atloo with No. 33131 from the University of Zanjan. The authors would like to thank various people for their contribution to this work, their valuable technical support on this work, and their help in the collection of plant data, and also all the technicians who helped in handling the instruments. Also, the authors gratefully acknowledge Zanjan University of Medical Sciences for this research work.

References

1. Bertram JS (2000) The molecular biology of cancer. Molecular aspects of medicine 21(6):167–223. https://doi.org/10.1016/C2013-0-07228-3
2. Schreiner L (2013) Innovative cancer therapeutics based on polymers or biogenic drugs evaluated in murine tumor models. Dissertation, LMU München. Diss. Lmu, Thesis. https://doi.org/10.5282/edoc.15618
3. Rahib L et al (2014) Projecting cancer incidence and deaths to 2030: the unexpected burden of thyroid, liver, and pancreas cancers in the United States. Cancer Res 74(11):2913–2921
4. Malam Y, Loizidou M, Seifalian AM (2009) Liposomes and nanoparticles: nanosized vehicles for drug delivery in cancer. Trends Pharmacol Sci 30(11):592–599
5. Xu T, Zhang N, Nichols HL, Shi D (2007) Modification of nanostructured materials for biomedical applications. Mater Sci Engineering: C 27(3):579–594
6. Park JW (2002) Liposome-based drug delivery in breast cancer treatment. Breast Cancer Res 4(3):95
7. Chen F-H, Zhang L-M, Chen Q-T et al (2010) Synthesis of a novel magnetic drug delivery system composed of doxorubicin conjugated Fe 3 O 4 nanoparticle cores and a PEG-functionalized porous silica shell. Chem Commun 46(45):8633–8635
8. Dobson J (2006) Magnetic nanoparticles for drug delivery. Drug Dev Res 67(1):55–60
9. Karami E, Behdani M, Kazemi-Lomedasht F (2019) Albumin nanoparticles as nanocarriers for drug delivery: Focusing on antibody and nanobody delivery and albumin-based drugs. Journal of Drug Delivery Science and Technology 55:101471
10. Jo Y-K et al (2017) Enhancement of the antitumor effect of methotrexate on colorectal cancer cells via lactate calcium salt targeting methionine metabolism. Nutr Cancer 69(4):663–673
11. Chen G et al (2016) Nanochemistry and nanomedicine for nanoparticle-based diagnostics and therapy. Chem Rev 116(5):2826–2885
12. Wang H et al (2002) Preparation of CuO nanoparticles by microwave irradiation. J Cryst Growth 244(1):88–94
13. Kose S et al (2012) Some physical properties of In doped copper oxide films produced by ultrasonic spray pyrolysis. Curr Appl Phys 12(3):890–895
14. Applerot G et al (2012) Understanding the antibacterial mechanism of CuO nanoparticles: revealing the route of induced oxidative stress. *Small* 8(21):3326–3337
15. Grigore M, Elena et al (2016) Methods of Synthesis, Properties and Biomedical Applications of CuO Nanoparticles. Pharmaceuticals 9:75
16. Nishino F et al (2017) Formation of CuO nano-flowered surfaces via submerged photo-synthesis of crystallites and their antimicrobial activity. Sci Rep 7:1–11
17. Wang J, Zhang B (2018) Bovine serum albumin as a versatile platform for cancer imaging and therapy. Curr Med Chem 25(25):2938–2953
18. Kratz F (2008) Albumin as a drug carrier: design of prodrugs, drug conjugates and nanoparticles. J Controlled Release 132(3):171–183
19. Ranucci E et al (1995) Modification of albumins by grafting poly (amido amine) chains. Polymer 36:2989–2994
20. Wongsasulak S et al (2007) The effect of solution properties on the morphology of ultrafine electrospun egg albumen–PEO composite fibers. Polymer 48(2):448–457
21. Jahanban-Esfahlan A, Roufegarinejad L, Jahanban-Esfahlan R, Tabibiazar M, Amarowicz R(2020) Latest developments in the detection and separation of bovine serum albumin using molecularly imprinted polymers. Talanta 207:120317
22. Wilken. R R, Veena. MS, Wang MB, Srivatsan ES (2011) Curcumin: a review of anti-cancer properties and therapeutic activity in head and neck squamous cell carcinoma. Mol Canc 10(1):12
23. Ahmed M et al (2018) Sulfonamides containing curcumin scaffold: Synthesis, characterization, carbonic anhydrase inhibition and molecular docking studies. Bioorg Chem 76:218–227
24. Jagetia G.C (2007) Radioprotection and radiosensitization by curcumin. Adv Exp Med Biol 595:301–320
25. Xie J et al (2017) Therapeutic nanoparticles based on curcumin and bamboo charcoal nanoparticles for chemo-photothermal synergistic treatment of cancer and radioprotection of normal cells. ACS Appl Mater Interfaces 9(16):14281–14291
26. Sadhukha T, Scott Wiedmann T, Panayam J (2014) Enhancing Therapeutic Efficacy through Designed Aggregation of Nanoparticles. Biomaterials 35(27):7860–7869